

星形成ゼミ

2017/04/14

SFN #290 56-60

工藤哲洋 (長崎大)

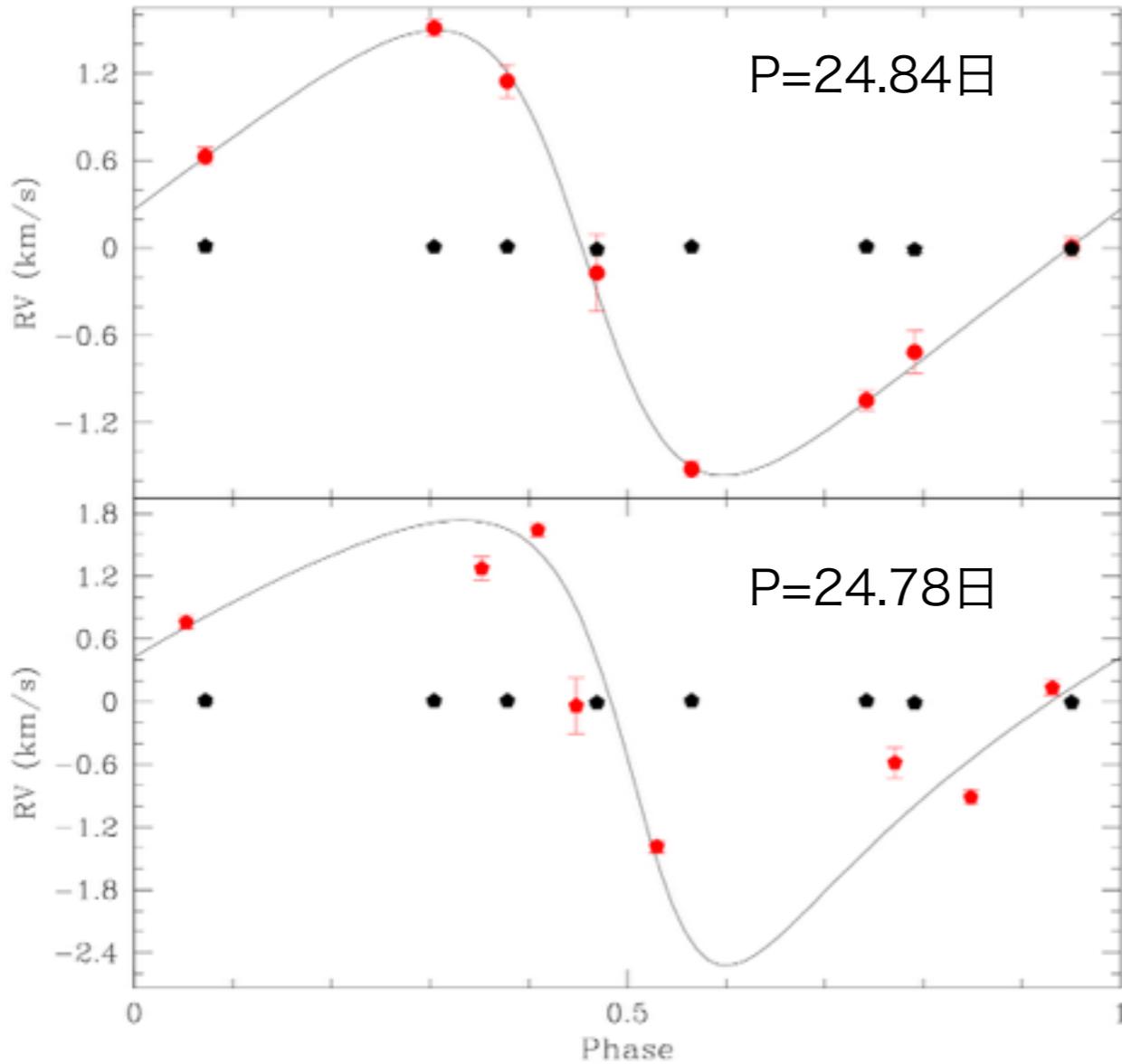
Evidence of a substellar companion around a very young T Tauri star ★

P. Viana Almeida^{1,3}, J. F. Gameiro^{2,3}, P. P. Petrov⁵, C. Melo⁴, N. C. Santos^{2,3}, P. Figueira^{2,3}, and S. H. P. Alencar¹

[arXiv:1701.02713](https://arxiv.org/abs/1701.02713)

- ・ T Tauri 星 AS205A (K5, $1 M_{\odot}$) の周囲に $19.25 M_J$ の伴星の証拠を発見した。長軸 0.17 AU 、離心率が 0.34 。(円盤の内縁 0.14 AU 。)
- ・ 元々、光度の観測から、 $P_1=6.78$ 日と $P_2=24.78$ 日の周期が観測されていた。(P_1 は自転と考えられる。)
- ・ 今回、近赤のドップラー効果で、 $P=24.84$ 日を発見した。

視線速度と位相



Orbital parameters	Value
P_{orb} (days)	24.84 ± 0.03
m_1 (M_{\odot})	0.9
$m_2 \sin i$ (M_{Jup})	19.25 ± 1.96
K (kms^{-1})	1.529 ± 0.16
e	0.34 ± 0.06
ω (deg)	94.14 ± 7.67
Semi-major axis (AU)	0.162 ± 0.04
V_{sys}	-10.25 ± 0.07
χ_{red}^2	1.07
$O - C$ (ms^{-1})	73.4

Table 2. Orbital parameters for the substellar companion.

確認するためにも，今後の視線速度の更なる観測が必要。

MID-INFRARED EXTINCTION AND FRESH SILICATE DUST TOWARDS THE GALACTIC CENTER

NIKOLAI V. VOSHCHINNIKOV,^{1,2} THOMAS HENNING³, AND VLADIMIR B. IL'IN^{1,4,5}

[arXiv:1701.08823](https://arxiv.org/abs/1701.08823)

- ・ 銀河中心の方向に生じる中間赤外の吸収線（3-8 μm に平らな吸収の特徴が見られるが原因不明）を説明するための、ダストモデルの提唱
- ・ 芳香族炭素の粒子，かんらん石タイプのケイ素の三層粒子，薄い多孔性の層，薄い磁鉄鉱の外層，を含むモデルが観測を説明する。
- ・ これらのダストは，銀河中心の晩期型星の大気で最近生成されたものである。

モデル番号表

20	93% a-Sil _{Fe} -7% cel1000 ($\mathcal{K} = 0.28$) / 73% optEC _(s) -27% cell1000	313.9	0.240	3.48	10.0	3.44	Fig. 4
21	93% olmg50-7% cel1000 ($\mathcal{K} = 0.19$) / 73% cel400-27% cell1000	90.1	0.391	2.99	9.8	3.35	
Three-layered spheres							
22	10% Fe-10% vac*-80% olmg50 ($\mathcal{K} = 0.77$) / cell1000	164.3	0.231	3.06	9.8	3.41	Fig. 2
23	10% vac-10% Fe-80% olmg50 ($\mathcal{K} = 0.18$) / cell1000	68.5	0.280	5.29	9.6	0.68	Fig. 2
24	98.99% olmg50-1% vac*-0.01% Fe ($\mathcal{K} = 0.09$) / cell1000	89.5	1.213	4.83	8.2	1.49	Fig. 2
25	90% olmg50-5% vac*-5% Fe ₃ O ₄ ($\mathcal{K} = 0.91$) / cell1000	6.7	0.696	3.22	9.8	3.45	Fig. 3, 4
26	90% olmg50-5% vac*-5% Fe ₂ O ₃ ($\mathcal{K} = 0.47$) / cell1000	31.7	0.332	3.56	9.8	2.39	Fig. 3
27	90% olmg50-5% vac*-5% FeO ($\mathcal{K} = 0.48$) / cell1000	36.2	0.319	3.51	9.8	2.21	Fig. 3
28	90% olmg50-5% vac*-5% FeS ($\mathcal{K} = 0.16$) / cell1000	94.3	0.319	4.42	9.8	0.61	Fig. 3
29	90% pyrimg50-5% vac*-5% Fe ₃ O ₄ ($\mathcal{K} = 0.72$) / cell1000	75.7	0.781	2.91	9.1	3.22	
Two-cloud model							
30	model 20 + model 25 (see Sect. 3.4)	84.9	0.468	3.32	9.9	3.41	Fig. 4

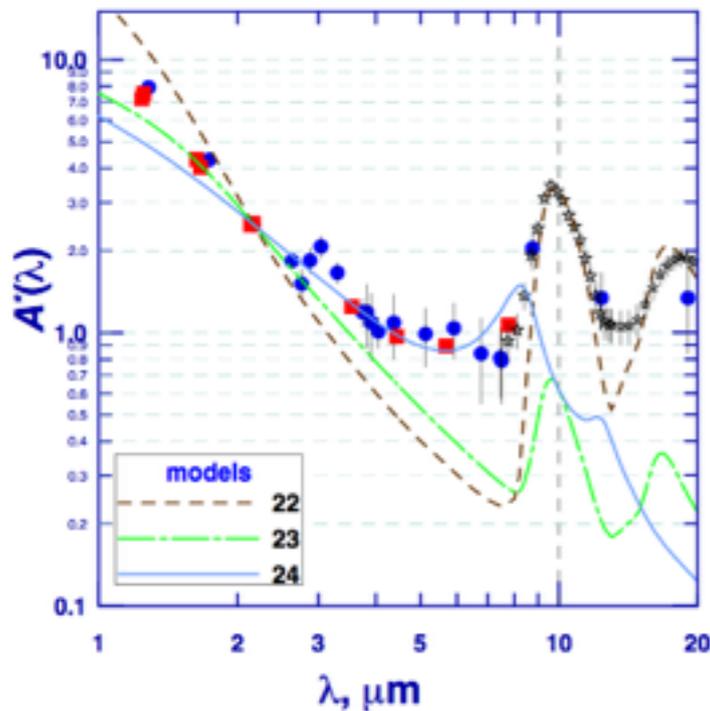


Figure 2. Same as Fig. 1 but for the models with mixtures of the three-layered silicate particles and homogeneous carbonaceous particles. Three-layered particles consist of olivine, iron and vacuum. Fe is located in the particle core (model 22), intermediate layer (model 23) or outer layer (model 24).

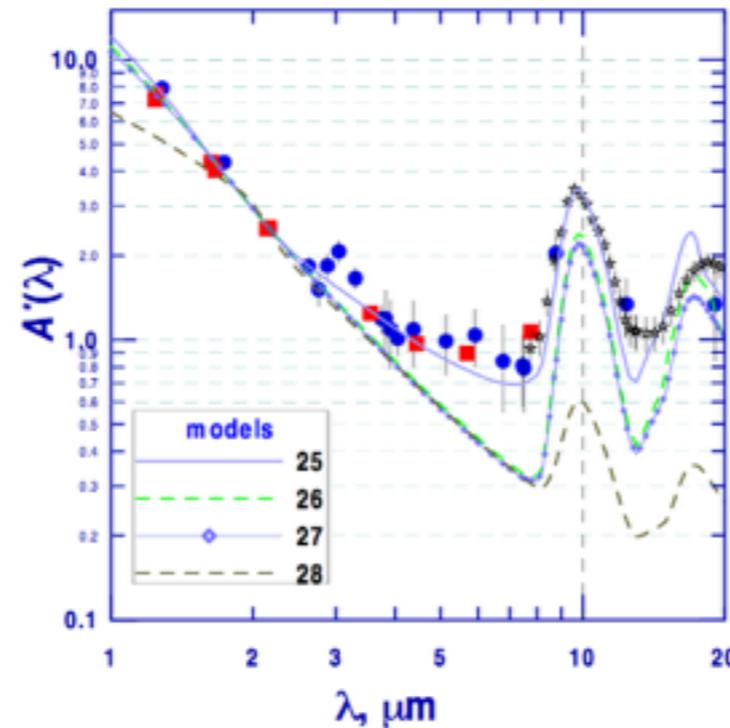


Figure 3. Same as Fig. 2 but for three-layered particles consisting of olivine (core), very porous intermediate layer and iron oxide or sulfide (outer layer). The outer layer is from Fe₃O₄ (model 25), Fe₂O₃ (model 26), FeO (model 27) or FeS (model 28).

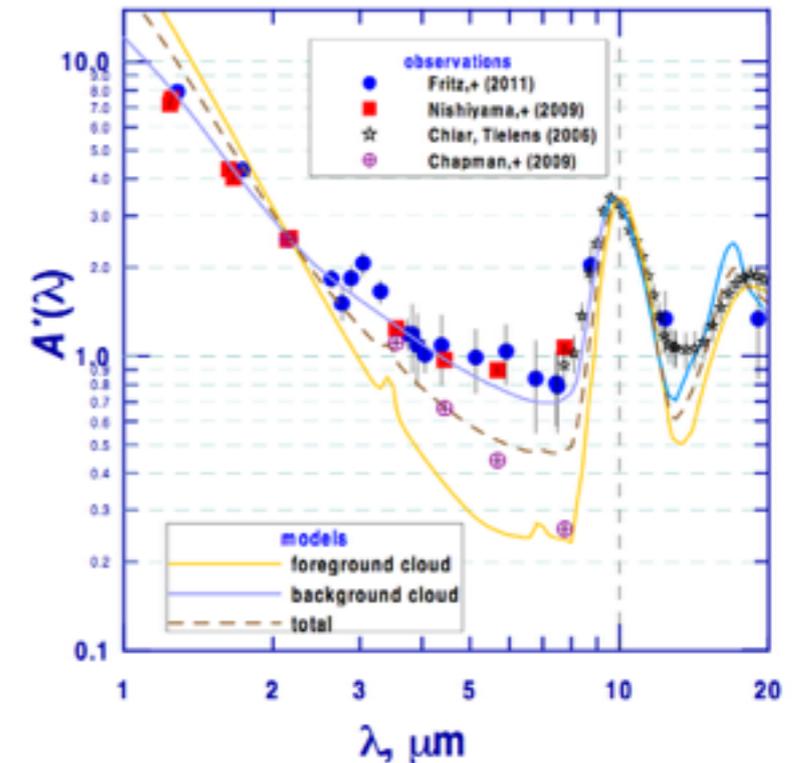


Figure 4. Comparison of the normalized IR extinction observed towards the Galactic Center (filled circles and squares) with that predicted by the model 20 with processed core-mantle particles in the foreground cloud and model 25 with fresh silicate 3-layered particles in the background cloud. Dashed brown line shows the total extinction produced in the foreground and background clouds as calculated from Equation (2). Crossed circles present the average wavelength dependence of the interstellar extinction for three molecular clouds in the local ISM (Chapman et al. 2009).

鉄がコアや内部にあるモデル(22,23)よりは、外層にあるモデル(24)が合う

Fe₃O₄が外層にあるモデル(25)が合う

ダストが遠方(銀河中心近く)にあるモデルが合う

AN ALMA AND MagAO STUDY OF THE SUBSTELLAR COMPANION GQ LUP B*

YA-LIN WU¹, PATRICK D. SHEEHAN¹, JARED R. MALES¹, LAIRD M. CLOSE¹, KATIE M. MORZINSKI¹, JOHANNA K. TESKE^{2,†}, ASHER HAUG-BALTZELL³, NIRAV MERCHANT^{3,4}, AND ERIC LYONS^{3,4}

[arXiv:1701.07541](https://arxiv.org/abs/1701.07541)

- ・ T Tauri星GQ Lupをこれまでにない高分解能の観測で調べた。 (GQ Lup : 10-40 M_Jの伴星 at 110 au)
- ・ 主星のダスト円盤は観測できたが、伴星は観測できなかった。 主星の円盤 : ~22AU, ~6M_{地球}, 傾斜角~56°
- ・ 主星の円盤の中にギャップは観測されなかった : 伴星を遠くに散乱した天体の形跡はなく、伴星は円盤の分裂か、星形成時の収縮で形成されたのだろう。

Table 1
GQ Lup のこれまでにわかっていた性質

Parameter	GQ Lup A	GQ Lup B	References
Distance (pc)	~150	~150	1, 2
Separation (")	...	0.721 ± 0.003	3
PA (°)	...	277.6 ± 0.4	3
Age (Myr)	2-5	2-5	4
SpT	K7eV	L1 ± 1	5, 6
A_V (mag)	0.4 ± 0.2	...	7
$\log(L/L_\odot)$	0.0 ± 0.1	-2.47 ± 0.28	4, 6
T_{eff} (K)	4300 ± 50	2400 ± 100	4, 6
Radius	$1.7 \pm 0.2 R_\odot$	$3.4 \pm 1.1 R_{\text{Jup}}$	4, 8
Mass	$1.05 \pm 0.07 M_\odot$	~10-40 M_{Jup}	4, 6, 9, 10, 11, 12
$\log \dot{M}$ ($M_\odot \text{ yr}^{-1}$)	-9 to -7	-12 to -9	3, 4, 13, 14, 15
$\log g$	3.7 ± 0.2	4.0 ± 0.5	4, 6
Inclination (°)	27 ± 5	...	16
$v \sin(i)$ (km s^{-1})	5 ± 1	$5.3^{+0.9}_{-1.0}$	4, 17
Rotation Period (d)	8.45 ± 0.20	...	16

Table 2
観測された円盤の物理量

Parameter	Model A	Model B
Dust Mass (M_\oplus)	5.9 ± 1.0	5.5 ± 0.8
Total Mass [†] (M_\oplus)	77.2 ± 8.4	76.8 ± 8.3
Inner Radius (AU)	1.5 ± 0.8	1.7 ± 1.1
Radius (AU)	23.8 ± 1.6	19.5 ± 1.4
h_0	0.084 ± 0.065	0.075 ± 0.039
γ	0.10 ± 0.22	-0.21 ± 0.20
β	1.26 ± 0.19	1.45 ± 0.25
Inclination (°)	56.2 ± 4.8	55.3 ± 6.0
PA (°)	348.8 ± 4.8	348.6 ± 5.0

[†] Total mass is calculated by adding our dust mass to the gas mass of $71.3 \pm 8.3 M_\oplus$ measured by MacGregor et al. (2017).

ALMA観測結果

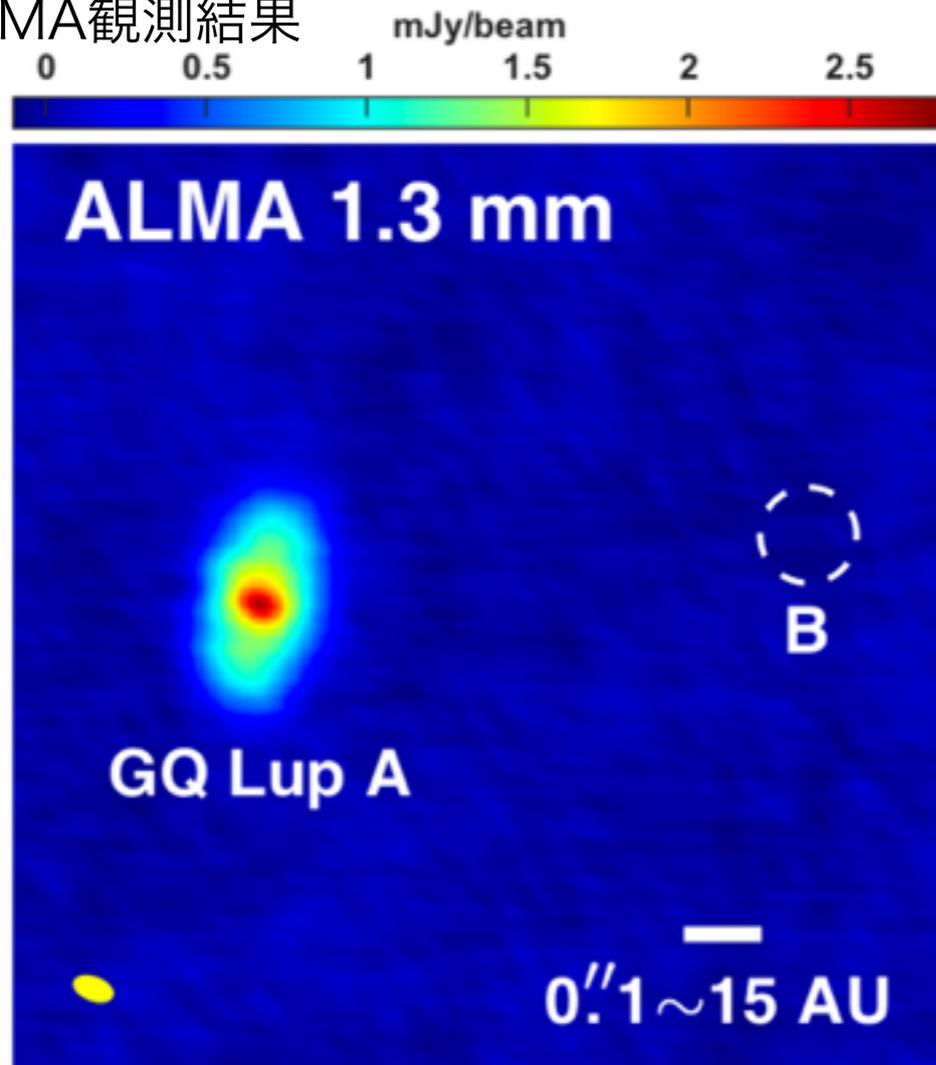


Figure 1. ALMA 1.3 mm continuum map showing GQ Lup A's accretion disk. We did not detect B's disk (dashed circle). The $0''.054 \times 0''.031$ beam (8.1 AU \times 4.7 AU at a distance of 150 pc) is shown as a yellow oval. North is up and east is left.

GQ Lup Bの形成に関する理論との比較

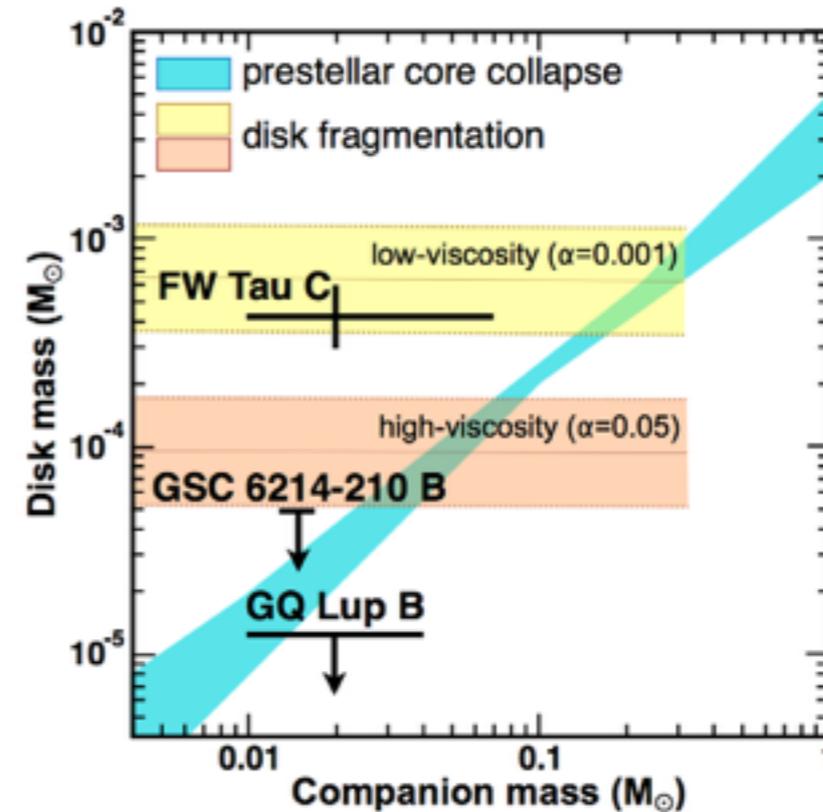


Figure 10. Mass of disk versus mass of companion for two formation pathways. Figure adapted from Stamatellos & Herczeg (2015). Turquoise area represents the best fits to the Taurus star-forming region in Andrews et al. (2013), without including the 0.7 dex of standard deviation. Yellow and salmon swaths are the $\pm 1\sigma$ intervals for 1 to 10 Myr objects formed by disk fragmentation. Disk masses for substellar companions are adopted from Kraus et al. (2015), Bowler et al. (2015), and MacGregor et al. (2017). GQ Lup B seems to be more consistent with the formation via prestellar core collapse.

MOLECULAR OUTFLOWS: EXPLOSIVE VERSUS PROTOSTELLAR

LUIS A. ZAPATA¹, JOHANNES SCHMID-BURGK²,
LUIS F. RODRÍGUEZ¹, AINA PALAU¹, AND LAURENT LOINARD¹

[arXiv:1701.07113](https://arxiv.org/abs/1701.07113)

- ・ 分子流のうち、爆発的なアウトフロー（2例：Orion KL, DR21）に関して、典型的な双曲分子流（HH211, DG Tau B）と比較することで、その性質を調べた。
- ・ 爆発的なアウトフローは空間分布が大きく異なる
 - 多くの細かいフィラメントで構成され等方的。
 - ハッブル則に似た速度の空間分布。
- ・ 爆発的なアウトフローはエネルギーや質量が大きい。

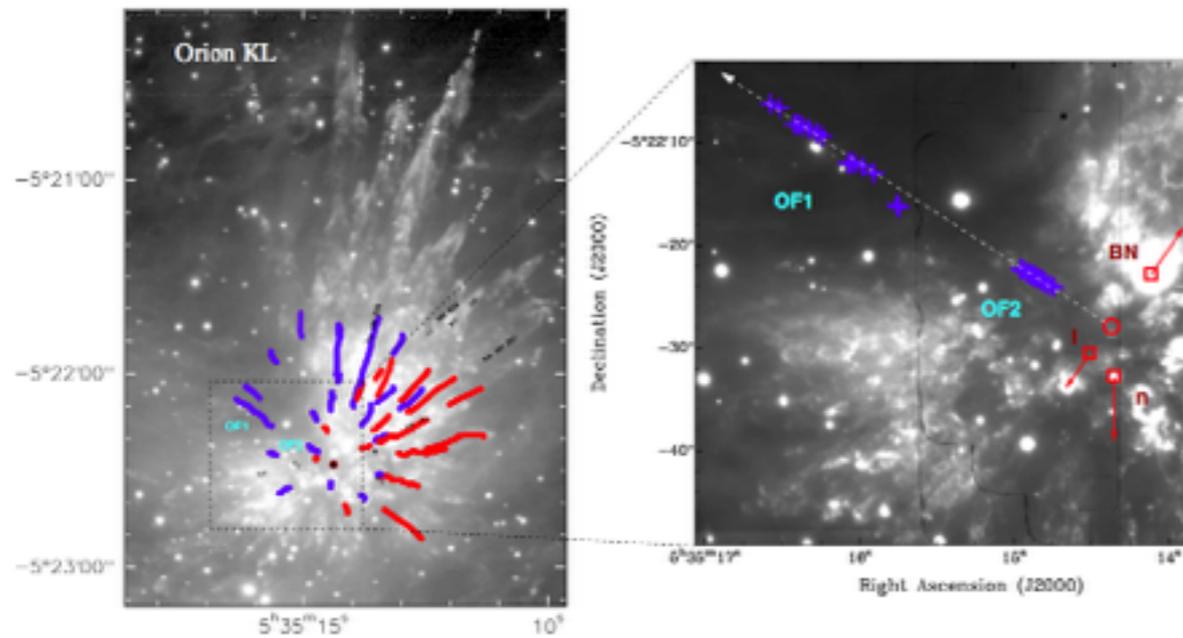
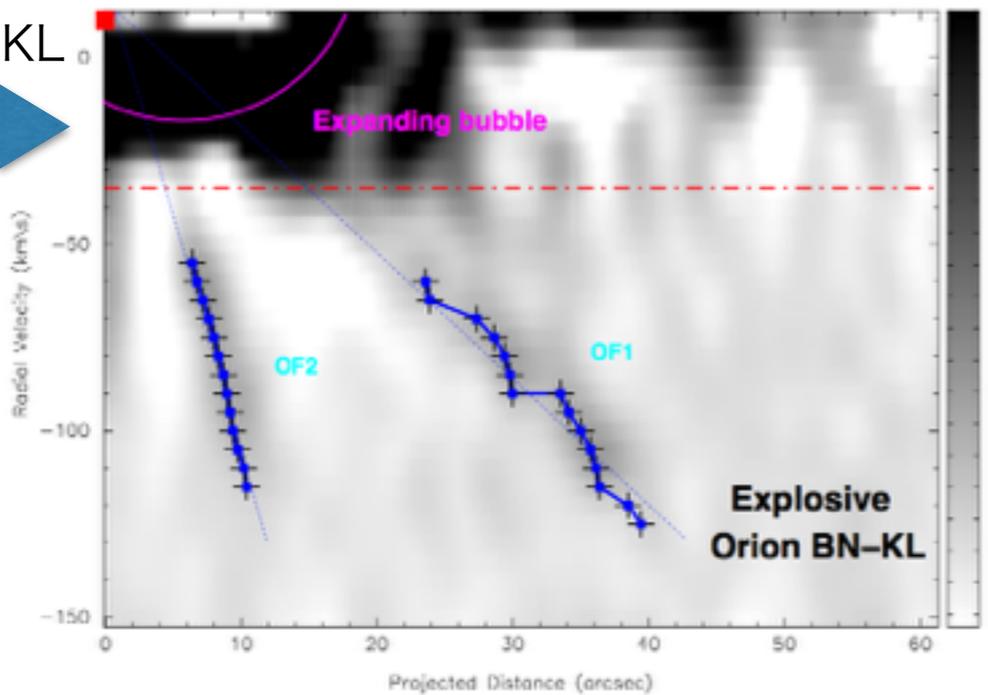


TABLE 1
PHYSICAL PARAMETERS OF THE EXPLOSIVE AND PROTOSTELLAR OUTFLOWS

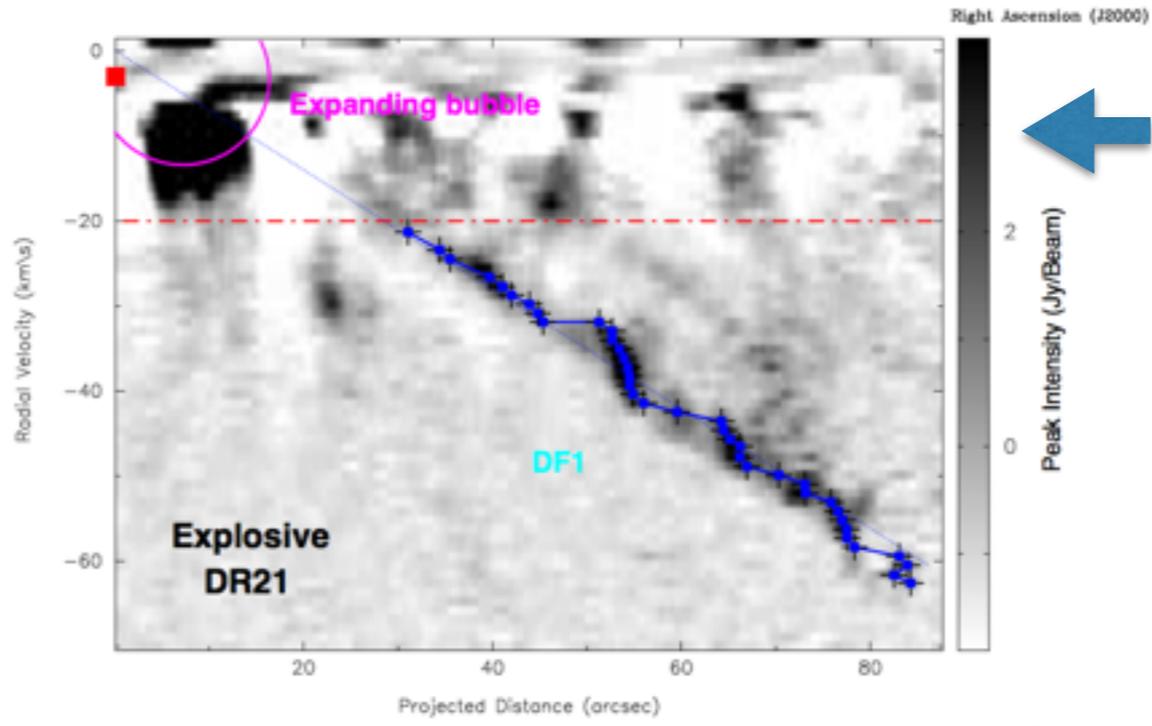
Name	Mass [M _⊙]	Mean Velocity [km s ⁻¹]	Momentum [M _⊙ km s ⁻¹]	Energy [10 ⁴⁵ erg]	Dynamical Age [years]	Mechanical Luminosity [L _⊙]
<i>Explosive Outflows (One single filament)</i>						
Orion KL ^a	≥ 0.12	70	8.4	5.9	~ 500	~ 93
DR21 ^b	≥ 0.51	40	20.5	8.2	~ 10 ⁴	~ 6.5
<i>Protostellar Low-mass Outflows</i>						
HH 211 ^c (blue lobe)	≥ 0.0015	20	0.03	0.006	3×10 ³	0.01
DG Tau B/ ^d	≥ 0.0025	20	0.05	0.01	700	0.1
<i>Protostellar Massive Outflows</i>						
IRAS 18162–2048-NW ^e	0.74	12.1	9	1.5	5×10 ³	2
IRAS 18360–0537 ^f (blue lobe)	27	15	405	55	8×10 ³	63

NOTE. — The physical parameters of all these outflows have been obtained with an (sub)millimeter interferometer. a). Parameters obtained from this work. The dynamical age is obtained from Zapata et al. (2009). b). Parameters obtained from this work. The dynamical age is obtained from Zapata et al. (2013a). c). Parameters obtained from Fernández-López et al. (2013). d). Parameters obtained from Qiu et al. (2012). e). Parameters obtained from this work. The dynamical age is obtained from Palau et al. (2006). f). Parameters obtained from Zapata et al. (2015).

Orion KL



同様に DR21



比較のため
HH211

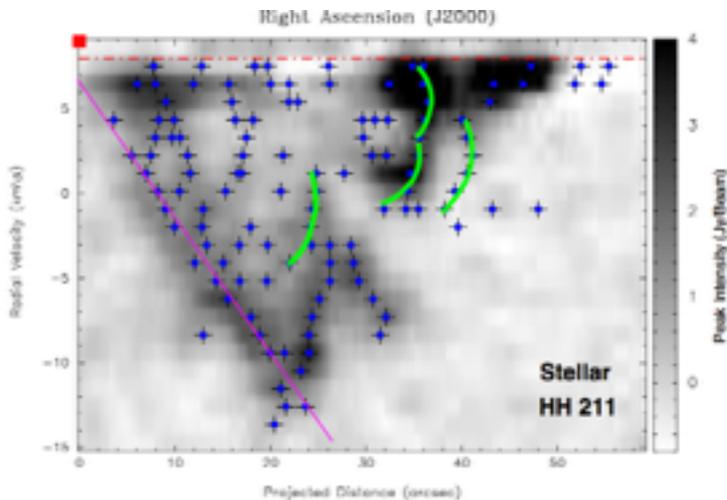


FIG. 3.— Upper Left Panel: H₂ infrared line image from the molecular outflow in Orion KL (Bally et al. 2011, 2015), overlaid with the SMA positions of the ¹²CO(J=2-1) red- and blueshifted compact condensations revealed in the spectral data cube (red and blue “filaments”) and reported in Zapata et al. (2009). All filaments point toward the same central position marked here with a red/black circle. Optical objects moving away from this center are shown as small arrows that indicate the direction of their motion (Doi et al. 2002; O’Dell et al. 2008). Right Panel: a zoom into the center of the outflow overlaid with the positions of the runaway sources BN, Source 1, and n, and the blueshifted “filaments” OF1 and OF2. The red arrows mark the the direction of the proper motion of the three runaway objects (Rodríguez et al. 2005; Gómez et al. 2005, 2008). The red circle represents the zone from where the three objects were ejected 500 years ago (Gómez et al. 2005). The dashed arrow marks the position of the cut shown in the lower panel and its orientation toward the positive values. Lower Position-velocity diagram of the two blueshifted ¹²CO(J=2-1) “filaments” called OF1 and OF2 (shown in the upper panel), overlaid with the positions of the compact condensations revealed in the spectral data cube (blue crosses), see Zapata et al. (2009). The PV diagram is made along a P.A. = 54°, see the upper panel. The red dashed line marks the position of the starting velocity range where the systemic velocity of the cloud is located. The emission inside of this range cannot be well sampled by the SMA. The red square indicates the position of the origin of the explosive outflow and its systemic velocity (~9.0 km s⁻¹; Zapata et al. 2009; Rodríguez et al. 2009). The truncated magenta circle shows part of the expanding molecular bubble reported in Zapata et al. (2011). The blue dashed lines trace the orientation of each filament.

Angular Momentum in Disk Wind Revealed in the Young Star MWC349A

Qizhou Zhang¹, Brian Claus¹, Linda Watson^{2,1}, James Moran¹

[arXiv:1702.02975](https://arxiv.org/abs/1702.02975)

- ・ H26 α とH30 α のメーザーでMWC349A (Herbig B[e])の円盤とアウトフローを観測した (SMA) .
- ・ それぞれ, 円盤成分からの放射とwind成分からの放射に分離できる. かつ, H26 α は中心星に対して内側, H30 α は外側から放射されている.
- ・ wind成分は回転を示している: 円盤からのwindとして角運動量を運んでいる強い証拠.

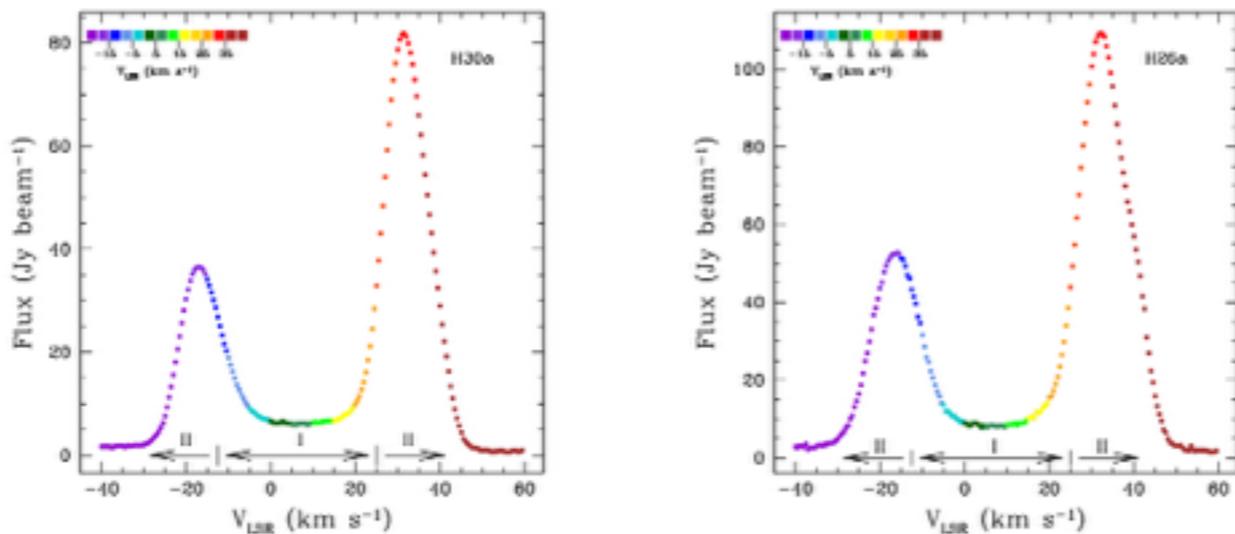


図2：視線速度と放射強度. グループIが円盤, グループIIがwindかの放射と解釈

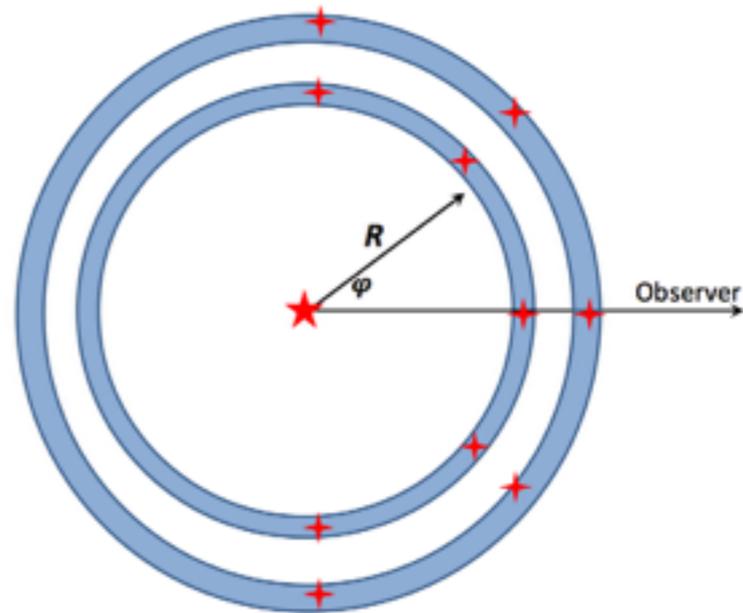


図5：結果解釈の概念図. 内側がH28α, 外側がH30α. エッジオンで見ている,

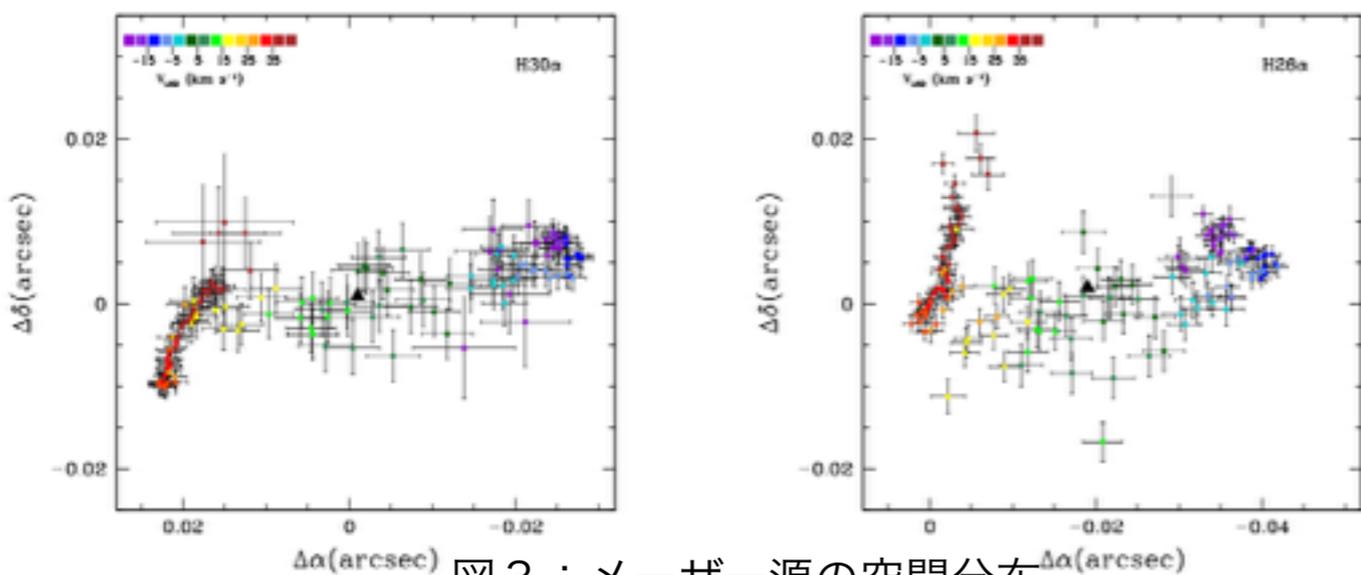


図3：メーザー源の空間分布

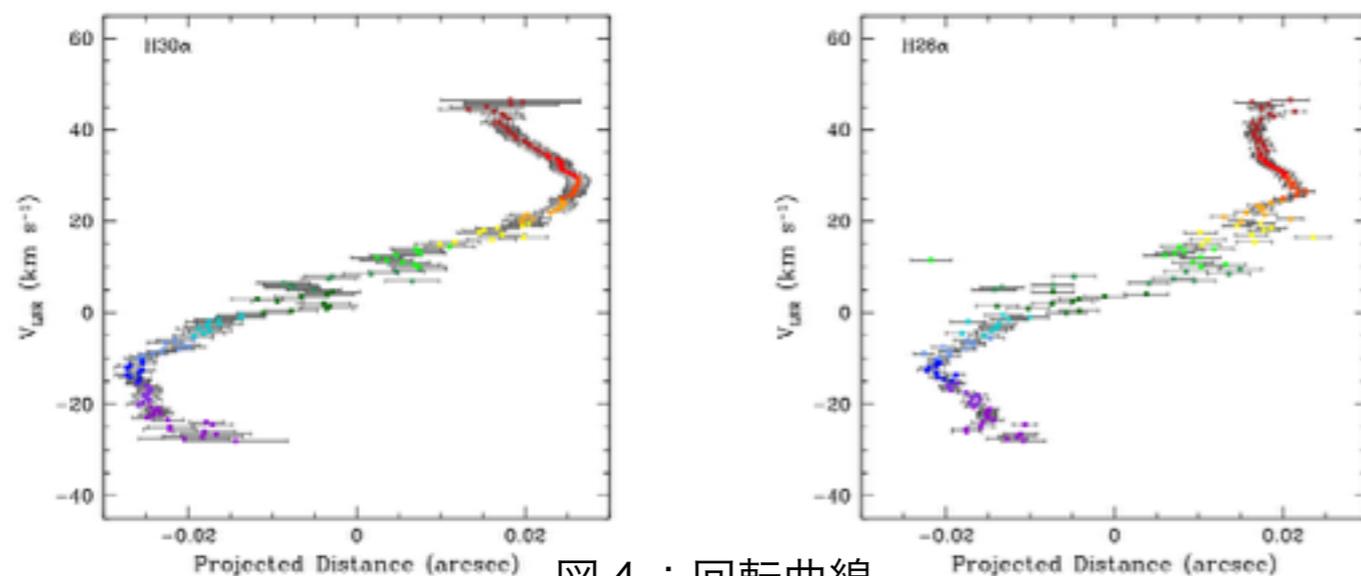


図4：回転曲線

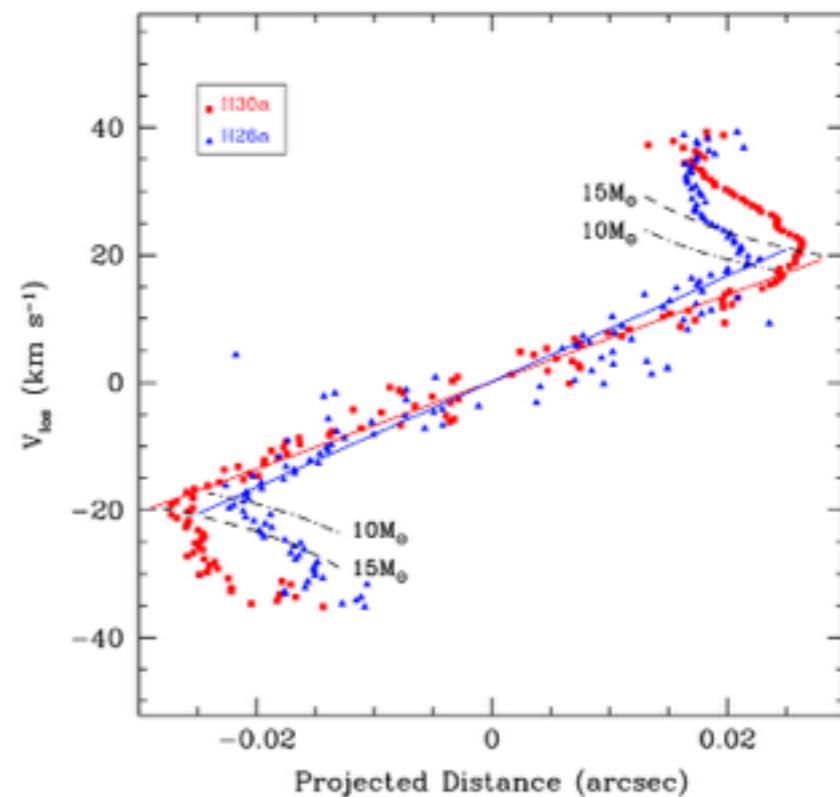


図6：回転曲線の比較